

Facile Preparation of Polyaniline Nanoparticles via Electrodeposition for Supercapacitors

Na Li, Yinghong Xiao, Chongzheng Xu, Huihui Li*, Xiaodi Yang*

Jiangsu Key Laboratory of New Power Batteries, School of Chemistry and Materials Science, Nanjing Normal University, Nanjing 210097, China;

*E-mail: huihuili@nynu.edu.cn; yangxiaodi@nynu.edu.cn

Received: 26 November 2012 / Accepted: 14 December 2012 / Published: 1 January 2013

A new facile synthesis method of polyaniline nanoparticles (PANI) by an in-situ electrodeposition was developed in this work. The morphologies of PANI nanoparticles could be controlled by the growth time in the electrodeposition process. The electrochemical supercapacitor properties of the PANI nanoparticles were examined using cyclic voltammetry (CV), electrochemical impedance spectroscopy (EIS), galvanostatic charge-discharge and cycling-life measurements. The PANI electrode composed of nanoparticles showed high specific capacitance (SC) value of $719 \text{ F}\cdot\text{g}^{-1}$ at a current density of $1 \text{ A}\cdot\text{g}^{-1}$ and high stability over 1000 cycles. The results of electrochemical measurements showed that these PANI nanoparticles have a potential application as the high-performance supercapacitor electrode material.

Keywords: polyaniline; nanoparticles; electrodeposition; supercapacitor

1. INTRODUCTION

The development of materials science has brought great momentum to applied electrochemical fields. Scientists in this field are always interested in finding new materials to improve electrochemical performances. Supercapacitors or electrochemical capacitors have gained a great attention in recent years because of their potential applications ranging from cellular phones to electric vehicles [1, 2]. These materials has the high electrical conductivity, good operational safety, and long cycling life as well as low cost and environmental friendliness [3].

Recently, as one of the ideal electrode materials, conducting polymers have attracted more and more attention in materials science for their unique electroactive properties and promising technological applications in energy storage [4~9]. Among the various conducting polymers, PANI has been applied extensively because of its facile synthesis and the controllable doping level which can be

achieved through an acid doping/base dedoping process [10]. Besides, PANI is inexpensive with good environmental stability, redox reversibility, and electrical conductivity [11~14]. The PANI-based supercapacitors could offer a high-performance and low-cost alternative source of energy to replace rechargeable batteries for various applications, such as electrical vehicles and high power tools [15].

There are various methods used to synthesize PANI, such as emulsions [16], template synthesis [17], self-assembly [18], and interfacial polymerization [19]. However, large amounts of surfactants are usually needed, which could make PANI difficult to attach the substrate without involving large contact resistance [20]. The electrochemical synthesis of PANI is simple and low-cost. The adherent films of PANI on the substrate can be easily prepared by the electrochemical deposition [21] and can be directly used for electrochemical studies.

In this paper, PANI nanoparticles were prepared by in-situ electrodeposition and were characterized by scanning electron microscopy (SEM) and Fourier transform infrared (FTIR) analysis. Electrochemical performance of PANI was evaluated by cyclic voltammetry (CV), electrochemical impedance spectroscopy (EIS), galvanostatic charge/discharge and cycling-life measurements. Its high conductivity, interesting electrochemical behavior and high electrochemical stability allow this material to be electrode materials for electrochemical supercapacitors.

2. EXPERIMENTAL

2.1. Apparatus and chemicals

Scanning electron microscopy (SEM) and Fourier transform infrared (FTIR) analysis were performed by JSM-5610LV scanning electron microscope (SEM, JEOL, Tokyo, Japan), NEXUS670 infrared ray spectrometer (FT-IR, Nicolet, USA), respectively. Electrochemical experiments were performed with a CHI660B electrochemical workstation (Chenhua Instrumental, Shanghai, China) using a three-electrode system composed of a glassy carbon electrode (GCE, 3mm diameter) as the working electrode, a platinum wire as the auxiliary electrode and an Ag/AgCl electrode as the reference electrode.

Aniline (analytical grade reagent, Xi'an Reagent Co, Xi'an, China) was freshly distilled under reduced pressure before use. Sulfuric acid (H_2SO_4 , 98%, Shanghai Chemical Reagent Co.), Nitric acid (HNO_3 , 68%, Shanghai Chemical Reagent Co.), Methanol (anhydrous, 99.8%, Sigma-Aldrich) and deionized water was used throughout the entire experiment (Resistance = $18.25 \text{ M}\Omega \cdot \text{cm}^{-1}$).

2.2. Procedure

The electrochemical measurements were carried out on CHI660B electrochemical working station at the ambient temperature. The GCE was polished with 1.0 μm , 0.3 μm , and 0.05 μm alumina powders and rinsed thoroughly with deionized water between each polishing step and sequentially sonicated in 1:1 HNO_3 , ethanol, and deionized water, and dried at room temperature. The electrolyte

was with H_2SO_4 (1.0 M) and aniline (0.3 M). PANI was electropolymerized on the surface of GCE at a constant potential of 0.75 V for various periods (300, 600, and 900 s), which were denoted as PANI-300s, PANI-600s and PANI-900s, respectively. After electrochemical growth, electrodes were washed with distilled water and dried.

3. RESULTS AND DISCUSSION

3.1 Surface morphological studies

To quantify the effect of the electrodeposition time on the PANI nanoparticles density and size, we used SEM to characterize the PANI nanoparticles surface under different electrodeposition time. Fig.1(A)-(C) present SEM images of the PANI-300s, PANI-600s and PANI-900s, respectively. The PANI-600s exhibited the highest room-temperature electrical conductivity among the polyaniline samples, which might be due to its unique structure. The image of PANI-600s (Fig.1B) seems to be uniform microporous on the surface and the particles were in nanometer scale. The average particle size of PANI-600s was found to be 50~100 nm. This is more useful to the electrolyte penetration in the charge-discharge process of the redox supercapacitor. Compared with that of PANI-300s and PANI-900s, PANI-600s had regular shapes and the porous nature of the nanoparticles. In addition, the image of PANI-600s showed better clearness than that of PANI-300s and PANI-900s. The electrochemical growth process of PANI is revealed to be similar to that of conventional growth of PANI [23]. It is well-known that the electrochemical polymerization of aniline mainly involved two stages [22]. First, a compact granular layer of PANI is formed on the bare electrode in the initial stage. Second, PANI further grows and then forms a loosely bound open structure in the advanced stage.

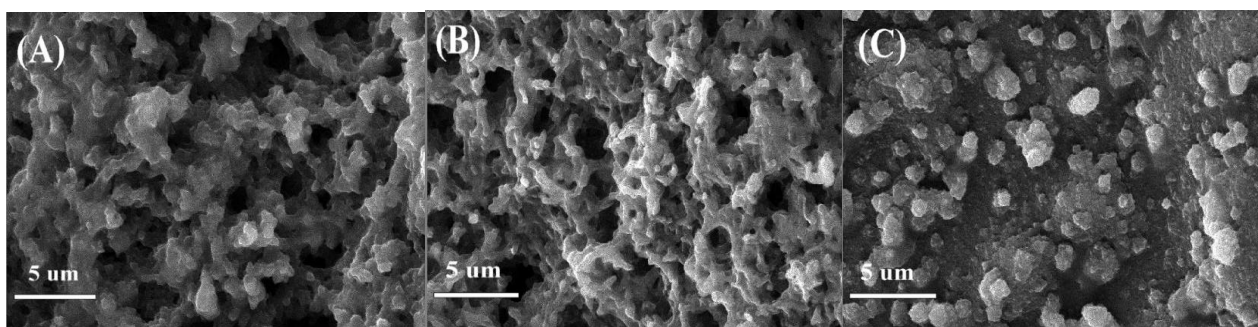


Figure 1. SEM images of the PANI-300s (A), PANI-600s (B), PANI-900s(C) modified electrodes.

3.2 FT-IR spectra analysis

FT-IR samples of PANI-600s nanoparticles were prepared by using KBr powder mixed and a force of 18 N using a pellet hydraulic press. Fig.2 shows the FTIR spectra of PANI-600s. The characteristic bands in the IR spectrum of PANI-600s occur at 3209, 2925, 1556, 1456, 1299, 1108, and 794 cm^{-1} . The band at 3209 cm^{-1} represents the N-H stretching modes. The one at 2925 cm^{-1} could be attributed to the C-N stretching of secondary aromatic amine (-N-benzenoid-N-), and the ones at

1556 and 1456 cm^{-1} are attributed to C=N and C=C stretching modes for the quinoid and benzenoid rings, respectively. The peaks at 1299 and 1108 cm^{-1} correspond to C-N stretching (-N-benzenoid-N-) and C=N stretching (-N=quinoid=N-), respectively [24, 25]. The band at 794 cm^{-1} is attributed to aromatic C-H bending out of the plane of the 1,4-disubstituted aromatic ring. The presence of all these vibrational modes clearly proved that polyaniline was successfully synthesized.

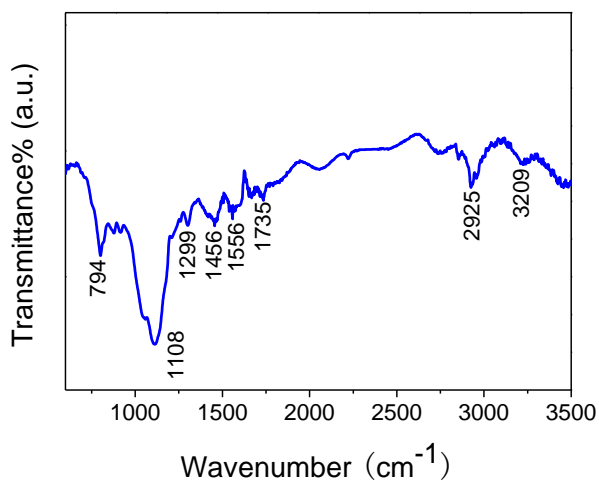


Figure 2. FTIR spectra of PANI-600 s.

3.3 Electrochemical characterization

3.3.1. Cyclic voltametry (CV)

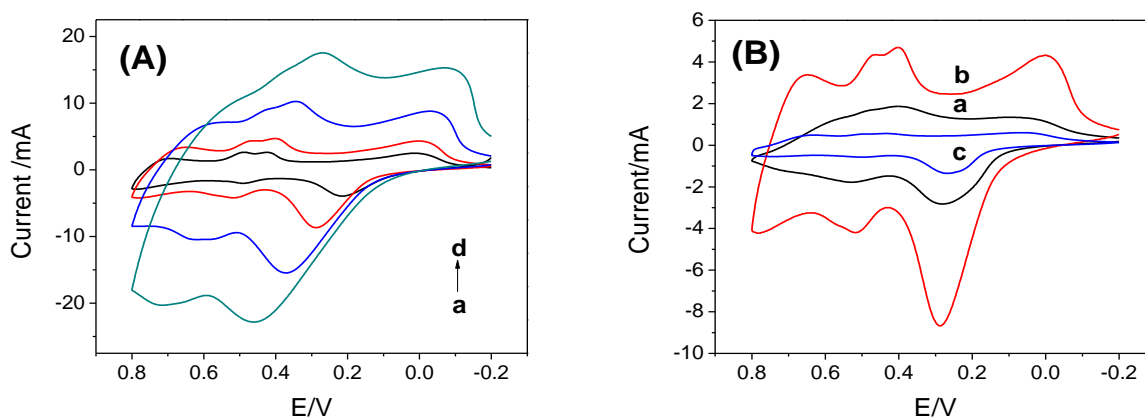


Figure 3. (A) Comparison of CVs scanned from -0.2 to 0.8 V in 1 M H_2SO_4 (aq) for the PANI-600s/GCE electrodes at scan rates of 10, 20, 50 and 100 $\text{mV} \cdot \text{s}^{-1}$ (from curve a to curve d). (B) Comparison of CVs for the PANI-300s, PANI-600s, and PANI-900s electrodes (from curve a to curve c) in 1 M H_2SO_4 (aq) at scan rate of 20 $\text{mV} \cdot \text{s}^{-1}$.

The cyclic voltammograms (CVs) of PANI-600s electrode recorded at different potential sweep rates from 10 to 100 $\text{mV}\cdot\text{s}^{-1}$ are presented in Fig.3(A). The CV data demonstrate the stability of the electrode within the applied potential range of -0.2 and 0.8 V. The near-rectangular-shaped CVs and high overall current revealed the perfect electrochemical capacitive behavior of PANI-600s electrode. The CVs for PANI-300s, PANI-600s, and PANI-900s electrodes at 20 $\text{mV}\cdot\text{s}^{-1}$ are shown in Fig.3(B). There is a clear symmetry in the redox peaks of PANI-600s, which indicates that both electron-transport and ion-diffusion rates in the PANI-600s are faster than that in PANI-300s and PANI-900s. The redox peaks for the PANI-600s were attributed to the redox transitions of PANI (i.e., the leucoemeraldine/emeraldine transition). Therefore, the capacitance of PANI-600s mainly comes from Faradaic reactions of PANI at the electrode/electrolyte surface [26].

3.3.2. Electrochemical impedance spectroscopy(EIS)

The significantly improved ion transport behavior of PANI-600s was further characterized using the electrochemical impedance spectroscopy (EIS) technique with a frequency range of 0.01 Hz-10 kHz in Fig.4. The amplitude of the applied sine wave potential was 5 mV, whereas the formal potential of the system was set at 0.2 V. EIS is a powerful technique complementary to the galvanostatic cycling measurement that provides more information on the electrochemical frequency behavior of the system. Compared with that of PANI-300s and PANI-900s, the Impedance Nyquist plot of PANI-600s had a semicircle in the high-frequency region, which was attributed to the process at the polymer/electrolyte interface [27]. This can be described by the double layer capacitance in parallel with the ionic charge-transfer resistance (R_{ct}). The high-frequency intercept of the semicircle on the real axis yielded the ohmic resistance (R_s), while the diameter provided R_{ct} of the electrode/electrolyte interface [28]. The negligible R_s for PANI-600s indicated a good electrode contact, which could be affected by charge transfer resistances and parallel faradaic resistances owing to pseudocapacitive materials.

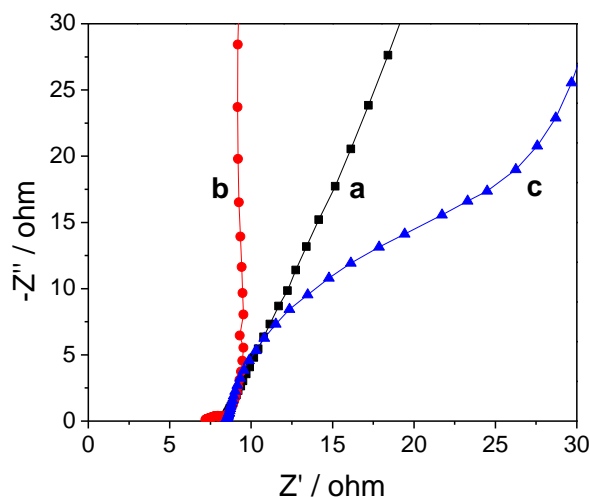


Figure 4. Impedance plot of PANI-300s(a), PANI-600s(b), PANI-900(c) electrodes in the frequency range of 0.01-10000 Hz in 1.0 M H_2SO_4 (aq).

3.3.3. Specific capacitance (SC)

To further confirm the merits of PANI-600s as supercapacitor electrodes, the electrochemical properties of PANI-600s was fully characterized by galvanostatic charge/discharge and cycling-life measurements. PANI-600s presented an excellent performance as supercapacitor electrode materials. Fig.5(A) shows the galvanostatic charge/discharge curve of PANI-600s after calculating the relative value. Near-ideal electric double-layer capacitance (EDLC) behavior of the curve could be observed with the highly linear charge and discharge slopes.

The specific capacitance of the PANI-600s electrode is calculated according to the following equation [4]:

$$C_m = \frac{It}{mV}$$

where C_m is the specific capacitance ($F \cdot g^{-1}$), m is the mass of the active materials in the device (g), V is 1 V, t is the discharge time and I is the charge/discharge current.

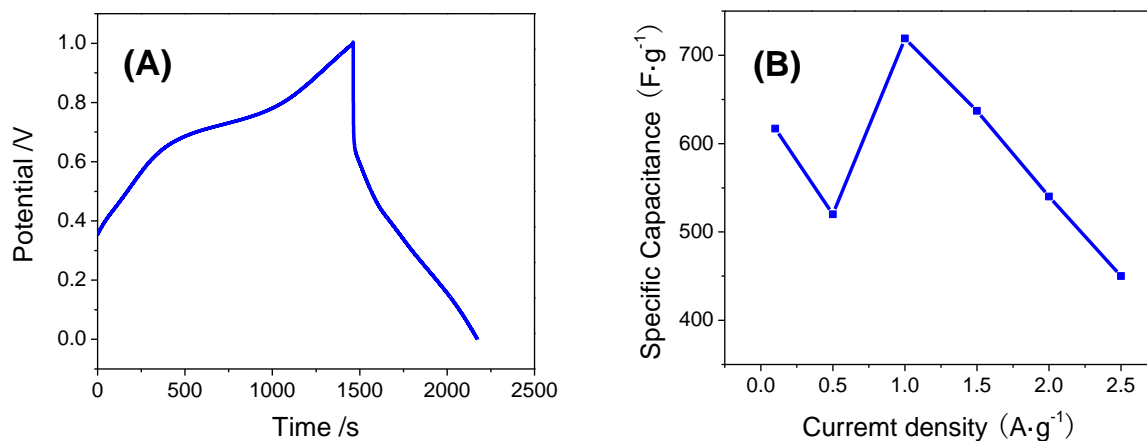


Figure 5. (A) The galvanostatic charge discharge curve for the PANI-600s electrode at a current density of $1 \text{ A} \cdot \text{g}^{-1}$ between 0 and 1.0 V versus Ag/AgCl in 1 M H_2SO_4 . (B) Specific capacitance as a function of current density for the PANI-600s electrode.

The specific capacitance of PANI-600s was found to be as high as $719 \text{ F} \cdot \text{g}^{-1}$ at a current density of $1 \text{ A} \cdot \text{g}^{-1}$. The excellent capacitive performance of the PANI-600s electrode can be clearly seen from in Fig.5(B). The value is much higher than those supercapacitors based on PANI prepared by other methods reported in the range of $160\text{-}500 \text{ F} \cdot \text{g}^{-1}$ [29, 30]. Its great capacitance might be due to its nanoparticle morphology. PANI nanoparticles with narrow diameters can shorten the charge-transport distance in the PANI materials, so the counterions easily penetrate the inner layer of PANI, which makes nearly full use of the electrode materials. Therefore, the ionic diffuse resistance and the charge-transfer resistance are reduced and the specific capacitance is substantially increased. The specific

gravimetric capacitances of samples under different current loads are summarized in Table 1. It is clear from Table 1 that the optimum current density was $1 \text{ A}\cdot\text{g}^{-1}$

Table 1. Specific Capacitance of PANI-600s at Different Current Densities

Current density ($\text{A}\cdot\text{g}^{-1}$)	0.1	0.5	1.0	1.5	2.0	2.5
Specific Capacitance ($\text{F}\cdot\text{g}^{-1}$)	617	520	719	637	541	452

3.3.4. Electrochemical stability of the PANI-600s electrode

Fig.6 shows the electrochemical stability of the PANI-600s/GCE at a current density of $1 \text{ A}\cdot\text{g}^{-1}$. During the initial 300 cycles, it is found that there is a gradual decrease in the SC value from 719 to $633 \text{ F}\cdot\text{g}^{-1}$. During 300 to 550 cycles, A little decrease could be observed. Up to 1000 cycles, the SC value remains fairly constant. The decrease in the SC value was to about 17% in 1000 cycles for PANI-600s. Therefore, the PANI nanoparticle electrode showed high stability and retained its electrochemical capacitance property over 1000 cycles.

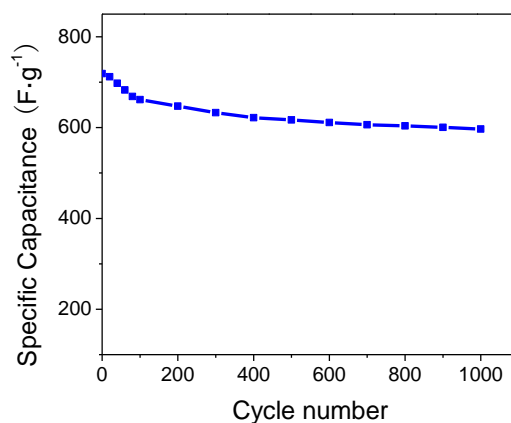


Figure 6. Cycling performance of the PANI-600s under a current density of $1 \text{ A}\cdot\text{g}^{-1}$.

4. CONCLUSIONS

In conclusion, we have presented a simple, rapid, and efficient electrochemical method to synthesize PANI nanoparticles by in-situ electrodeposition. Compared with PANI-300s and PANI-900s, these prepared PANI-600s nanoparticles seem to be uniform microporous on the surface, which can promote remarkable enhancement in the performance of supercapacitors. Specific capacitance of PANI-600s was obtained as high as $719 \text{ F}\cdot\text{g}^{-1}$. This prepared PANI nanoparticle electrode also showed high stability and retained its electrochemical capacitance property up to 1000 cycles. The high SC and the great cycle ability of PANI nanoparticle electrode coupled with the low cost and environmentally

benign nature could make them attractive for supercapacitor applications. Therefore, this synthesis method of PANI can be extended to the preparations of other conducting polymer nanoparticles.

ACKNOWLEDGEMENTS

The project is supported by the National Science Foundation of China (Grant Nos. 20902048, 20875047), Ministry of Water Resources (201201018) and the Priority Academic Program Development of Jiangsu Higher Education Institutions.

References

1. S. R. P. Gnanakan, M. Rajasekhar and A. Subramania, *Int. J. Electrochem. Sci.*, 4 (2009) 1289.
2. Q. Cheng, J. Tang, J. Ma, H. Zhang, L.C. Qin, *J. Phys. Chem. C.*, 115 (2011) 23584.
3. M. Q. Xue, F. W. Li, J. Zhu, H. Song, M. N. Zhang and T. B. Cao, *Adv. Funct. Mater.*, 22(2012) 1284.
4. Y. G. Wang, H. Q. Li, Y. Y. Xia, *Adv. Mater.*, 18 (2006) 2619.
5. S. Liu, J. Q. Wang, J. F. Ou, J. F. Zhou, Y. F. Chen and S. R. Yang, *J. Nanosci. Nanotechnol.*, 10 (2010) 933.
6. L. Q. Mai, F. Yang, Y. L. Zhao, X. Xu, L. Xu, Y. Z. Luo, *Nat. Commun.*, 2 (2011) 381.
7. Y. Zhu, S. Murali, M. D. Stoller, K. J. Ganesh, W. Cai, *Science*, 332 (2011) 1537.
8. Y. F. Yan, Q. L. Cheng, G. C. Wang, C. Z. Li, *J. Power Sources.*, 196 (2011) 7835.
9. M. R. Nabid, M. Golbabaee, A. B. Moghaddam, R. Dinarvand, R. Sedghi, *Int. J. Electrochem. Sci.*, 3 (2008) 1117.
10. Q. L. Hao, H. L. Wang, X. J. Yang, L. D. Lu and X. Wang, *Nano Res.*, 4 (2011) 323.
11. S. Bhadra, D. Khastgir, N. K. Sinha and J. H. Lee, *Prog. Polym. Sci.*, 34 (2009) 783.
12. S. K. Chen, J. F. Zhu, T. G. Zhou, B. He, W. Z. Huang, B. C. Wang, *Int. J. Electrochem. Sci.*, 7 (2012) 8170.
13. H. Y. Mi, X.G. Zhang, X.G. Ye, S. D. Yang, *J. Power Sources.*, 176(2008) 403.
14. H. Y. Mi, X. G. Zhang, S. Y. An, X. G. Ye, S. D. Yang, *Electrochem. Commun.*, 9 (2007) 2859.
15. J. M. Tarascon, M. Armand, *Nature*, 414 (2001) 359.
16. Z. Wei, M. Wan, *Adv. Mater.*, 14 (2002) 1314.
17. Z. Niu, Z. Yang, Z. Hu, Y. Lu, C. C. Han, *Adv. Funct. Mater.*, 13 (2003) 949.
18. H. J. Qiu, M. X. Wan, B. Matthews, L. Dai, *Macromolecules*, 34 (2001) 675.
19. J. X. Huang, R. B. Kaner, *J. Am. Chem. Soc.*, 126 (2004) 851.
20. V. Gupta, N. Miura, *Mater. Lett.*, 60 (2006) 1466.
21. S. K. Mondal, K. Barai, N. Munichandraiah, *Electrochim. Acta.*, 52 (2007) 3258.
22. Z. Mandić, L. Duić, F. Kovačiček, *Electrochim. Acta.*, 42 (1997) 1389.
23. H. Zhang, J. Wang, Z. Wang, F. Zhang, S. Wang, *Synth. Met.*, 159 (2009) 277.
24. M. Trchová, I. Šeděnková, E. Tobolková, J. Stejskal, *Polym. Degrad. Stabil.*, 86 (2004) 179.
25. A. H. Elsayed, M. S. Mohy Eldin, A. M. Elsyed, A. H. Abo Elazm, E. M. Younes and H. A. Motaweh, *Int. J. Electrochem. Sci.*, 6 (2011) 206.
26. J. J. Xu, K. Wang, S. Z. Zu, B. H. Han, Z. X. Wei, *ACS Nano*, 4 (2010), 5019.
27. W. C. Chen, T. C. Wen, C. C. Hu, A. Gopalan, *Electrochim. Acta.*, 47 (2002) 1305.
28. J. B. Zang, Y. H. Wang, X. Y. Zhao, G. X. Xin, S. P. Sun, X. H. Qu, *Int. J. Electrochem. Sci.*, 7 (2012) 1677.
29. D. S. Dhawale, A. Vinu and C. D. Lokhande, *Electrochim. Acta.*, 56 (2011) 9482.
30. H. Guan, L. Z. Fan, H. C. Zhang, and X. H. Qu, *Electrochim. Acta.*, 56 (2010) 964.